JOURNAL OF MATERIALS SCIENCE 21 (1986) 39–45

Effects of rubbery phase and absorbed water on impact-modified nylon 66

Part 2 *Fractography*

M. T. HAHN*, R. W. HERTZBERG, J. A. MANSON
Materials Research Center, Lehigh University, Bethlehem, Pennsylvania 18015, USA

The fracture surface micromorphology of nylon 66 and its blends was examined. A patchy appearance, found at low ΔK values when levels of imbibed moisture and impact modifier are low, is believed to result from a void coalescence mechanism. At higher water contents and levels of impact-modification, the fracture surface assumes a rumpled appearance with numerous secondary fissures oriented normal to the crack direction; the inter-rumple spacings, however, do not correspond to the macroscopic growth rate. A model to explain rumple formation is presented. The fatigue fracture surface appearance of unmodified nylon 66 is found to depend on both moisture content and test temperature. Trans-spherulitic fracture is found when the test temperature is below the glass transition temperature T_g (measured at 110 Hz) for a given water content, while at higher test temperatures a high degree of drawing is evident. It is concluded that the fracture surface micromorphology of nylon 66 and its blends depend strongly on the viscoelastic state of the polymer.

1. Introduction

Fractographic examination of fracture surfaces produced during fatigue is a valuable complement to studies designed to characterize material properties under cyclic loading conditions. For example, much progress toward understanding the fatigue crack growth process in amorphous plastics has been based on extensive fractographic investigations of fatigue striations and discontinuous growth bands (DGB) [1, 2]. The spacing between these fracture surface markings depends strongly on the stress intensity factor range ΔK; the striations correspond to the increment of crack advance resulting from one loading cycle, while the DGBs are associated with intermittent growth bursts after the crack remains dormant for many loading cycles.

Fewer fractographic studies of fatigue damage have been conducted for the case of semi- crystalline solids [3–6] though both striations and DGB markings have been reported in such materials as nylon 66 and polyacetal [4, 7]. More recently White and Teh [5] and Bretz *et al.* [6] examined the fracture surface micromorphology in several semi-crystalline polymers and observed features related to the original spherulitic structure. At low ΔK levels in dry nylon 66 and polyacetal, the crack tended to cut across spherulites rather than progress around the spherulite perimeter. (Friedrich [8] observed, under static loading conditions, both trans- spherulitic and interspherulitic crack growth in polypropylene specimens that possessed large- diameter spherulites.) At higher ΔK levels White and Teh [5] and Bretz *et al.* [6] reported fracture surface markings that corresponded to the "smearing-out" of the spherulites in the direction of the propagating fatigue crack.

Recent studies have focused on the fatigue crack propagation (FCP) behaviour of impact- modified nylon 66 blends [9–12]. These materials have superior toughness and excellent fatigue resistance. The objective of this paper is to correlate the fractographic appearance of these blends with the underlying microstructure of the material and with the macroscopic fatigue crack growth rates.

2. Experimental procedure

Impact-modified nylon blends were prepared by E. I. duPont de Nemours & Co. by combining varying amounts of nylon 66 (Zytel 101) with a commercially available blend (Zytel ST801, referred to hereinafter as HI–N66). The latter consists of a nylon 66 matrix with approximately 20% by weight of a modifier apparently based on a modified ethylene–propylene diene monomer (EPDM) elastomer in the form of dispersed submicron spherical particles [10]. For these studies, blends containing 25, 50 and 75% HI–N66 were prepared and fatigue-tested along with neat N66 and HI–N66 starting materials. Fatigue crack propagation testing procedures are described elsewhere [12]. Fatigue experiments also included an examination of the influence of water content in the blends on fatigue properties and fracture processes. The procedures for adding water to the blends are described elsewhere [3, 10].

Fracture surfaces were studied using an ETEC Autoscan scanning electron microscope (SEM) at an accelerating voltage of 20 kV. Specimens were

**Present address* Advanced Technologies Division, General Research, Santa Barbara, California 93160, USA.

0022–2461/86 $03.00 + .12

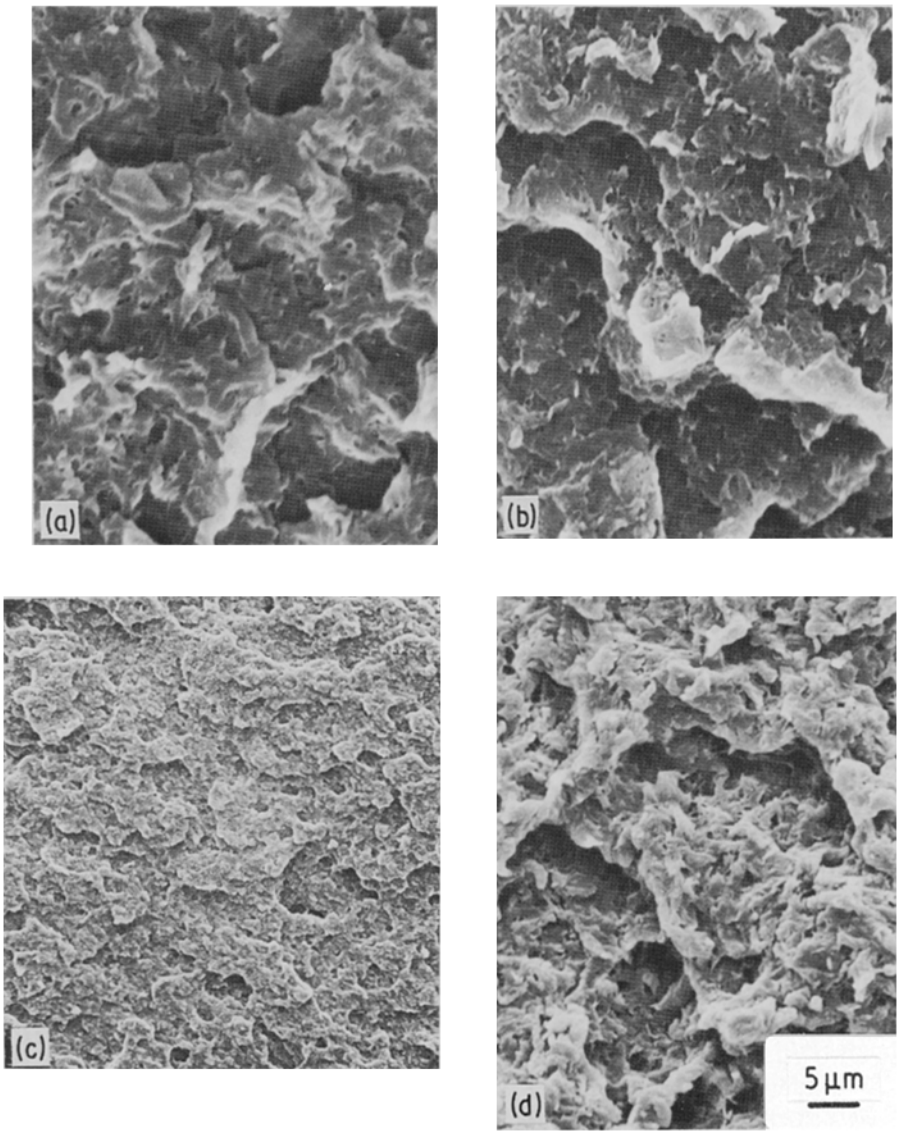

Figure 1 SEM fractographs of dry as-moulded HI–N66 blends illustrating patchy fracture morphology at $f = 10$ Hz. (a) 25% HI–N66, $\Delta K = 2.5\,\mathrm{MPa\,m^{1/2}}$, $da/dN = 1.0 \times 10^{-4}\,\mathrm{mm\,cycle^{-1}}$; (b) 50% HI–N66, $\Delta K = 2.3\,\mathrm{MPa\,m^{1/2}}$, $da/dN = 2.6 \times 10^{-5}\,\mathrm{mm\,cycle^{-1}}$; (c) 75% HI–N66, $\Delta K = 2.8\,\mathrm{MPa\,m^{1/2}}$, $da/dN = 1.98 \times 10^{-5}\,\mathrm{mm\,cycle^{-1}}$. (d) 100% HI–N66, $\Delta K = 2.8\,\mathrm{MPa\,m^{1/2}}$, $da/dN = 4.3 \times 10^{-5}\,\mathrm{mm\,cycle^{-1}}$.

mounted on aluminium stubs and sputter-coated with a gold–palladium alloy prior to examination.

3. Results and discussion

Correlation of fractographic observations with the microstructure of the material and the FCP behaviour provides insight into the deformation and fracture processes of these materials. In the HI–N66 blends, two basic fatigue fracture processes are observed on fracture surfaces that exhibit stress whitening, regardless of water content. At low stress intensities a "patchy" fracture surface is characteristic (Fig. 1); as the stress intensity increases, the fracture surface gradually transforms from the patchy to a "rumpled" appearance (Fig. 2). (In these and other micrographs the arrow indicates the direction of crack growth.)

Two morphologies are observed in the fast fracture region as well. In the dry as-moulded blend containing 25% HI–N66 there is a brittle fast fracture appearance, as shown in Fig. 3. The chevron-like fracture markings, which consist of radial lines emanating from a nucleating site in the middle of the figure,

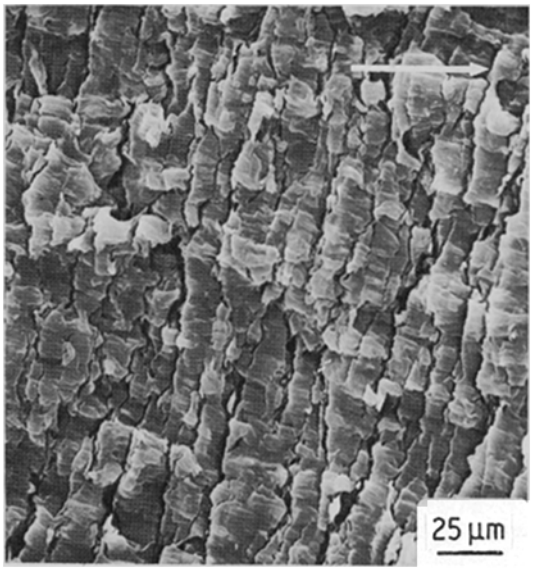

Figure 2 SEM fractograph of 50% HI–N66 illustrating typical "rumpled" fracture surface observed in fatigue of impact-modified nylon at high stress intensities. $\Delta K = 5.8\,\mathrm{MPa\,m^{1/2}}$, $da/dN = 7.8 \times 10^{-3}\,\mathrm{mm\,cycle^{-1}}$, $f = 10$ Hz.

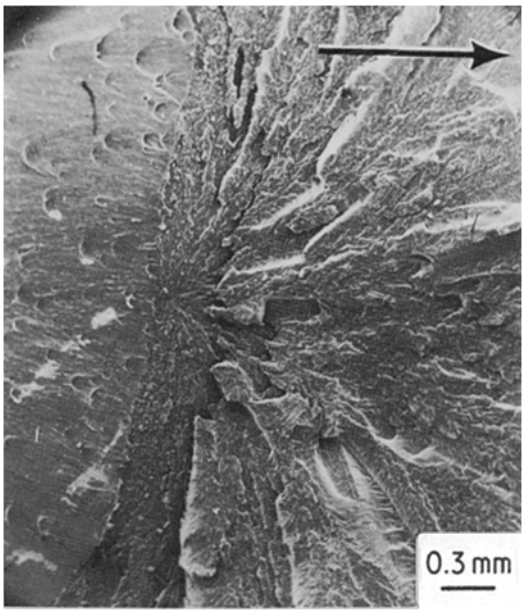

Figure 3 SEM fractograph of dry as-moulded 25% HI–N66 illustrating brittle fast fracture.

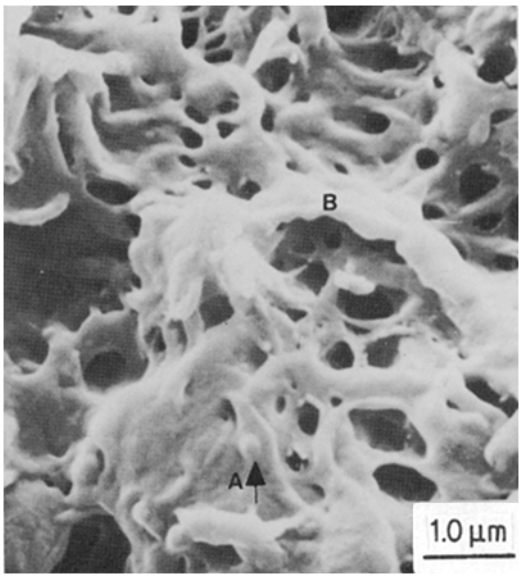

Figure 5 High-magnification view of patchy fracture surface in dry as-moulded 100% HI–N66. Note network of voids. Bumps suspected to be rubber particles are also seen, for example at A and B. $\Delta K = 3.0\,\mathrm{MPa\,m^{1/2}}$, $da/dN = 1.0 \times 10^{-4}\,\mathrm{mm\,cycle^{-1}}$, $f = 10\,\mathrm{Hz}$.

resemble those which occur in dry as-moulded neat nylon 66 [3]. The fracture planes bounded by the radial lines (actually fracture ledges) coalesce as the crack proceeds (from left to right in Fig. 3). Macroscopic crack branching occurs occasionally during rapid unstable fracture, thereby causing the sample to break into three or more pieces. With both the dry blend containing 25% HI–N66 and the dry neat nylon 66, the fast fracture occurs without associated stress- whitening.

In all other samples, including the blend containing 25% HI–N66 with at least 1% absorbed water, the final fracture zone exhibited considerable stress whitening and was generated by a tearing process during the last few loading cycles of the specimen. In this regime, the applied load range tended to decrease as the specimen compliance increased. This type of fast fracture produced a rumpled fracture surface

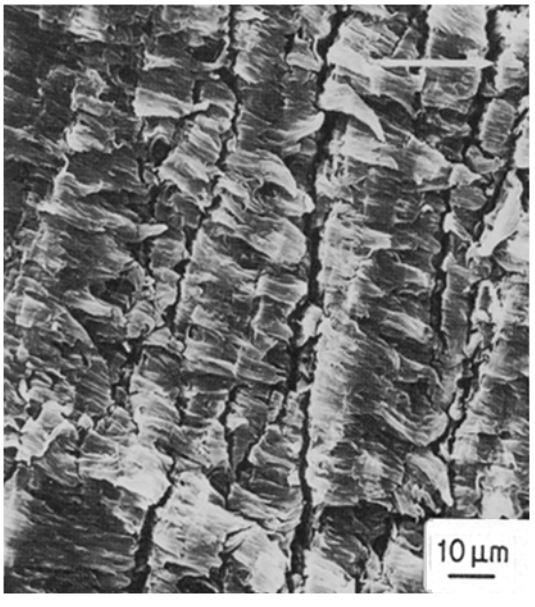

Figure 4 SEM fractograph of dry as-moulded 50% HI–N66 illustrating fast fracture. Note drawing of material across the fissures.

appearance (Fig. 4), which differs from the comparable fatigue fracture surface morphology (Fig. 2) in that the rumples are less sharply-defined and the material experiences considerable drawing which further obscures the rumples.

The fatigue fracture surface micromorphology of the patchy region is now examined in greater detail (Fig. 1). Viewing the fracture at higher magnification reveals many small voids and bumps as noted in Fig. 5. Since the bumps are the same size as the rubber particles and increase in number in blends richer in HI–N66, it is quite possible that they are a consequence of the involvement of the reinforcing phase in the fracture process. If the bumps are rubber particles, they indicate that the fracture occurs often at the particle–matrix interface. Unfortunately, it was not possible to unequivocally confirm the presence of the rubber particles on the fracture surface. In principle, osmium tetroxide staining and subsequent X-ray analysis of the fracture surface could determine whether the bumps are rubber particles. However, since the X-ray excitation volume is of the order of 5 μm in diameter, it is considerably larger than the volume of a single rubber particle. Hence, the excited volume could "see" particles lying below the fracture surface as well as those on the fracture surface.

What is the origin of the patchy fracture surface morphology? In FCP of unmodified nylon 66, Bretz *et al* [4] observed a patchy morphology, superficially similar in appearance to that seen here in the modified nylon. They found that the patch size and the spherulite size were both 10 to 20 μm. Moreover, the radial morphology of the patches suggested transspherulitic fracture with retention of the spherulite morphology. It was initially thought that a similar fracture process occurred in the modified nylon, but on closer examination this does not appear to be the case. On the fracture surfaces in Fig. 1a to d are

patches (10 to 20 μm in size) which are much larger than the observed spherulite size (0.5 to 2 μm) [10]. However, the finer structure observed at higher magnification, as shown in Fig. 5, reflects the effects of a different fracture process. This fine structure has a spongy, porous appearance and consists of interconnected voids.* Comparing Fig. 5 with thin film sections viewed in the transmission electron microscope [10], the spacing of the voids is observed to be roughly the same as the spacing between the rubber particles. This suggests that fatigue damage occurs by microvoid nucleation at the rubber particles and by the subsequent growth and coalescence of these voids. The greater density of voids in the richer blends corresponds to the greater density of rubber particles, and hence of void nucleation sites. Void nucleation is believed to occur by debonding of the rubber particles at the rubber–nylon interface, which is favoured by dilatational stresses in the nylon caused by the differences in Poisson's ratio between the nylon and the rubber. The more-rounded appearance of the fracture surfaces in the richer blends is apparently due to their greater ductility, especially in view of the greater crack-tip temperatures experienced in the richer blends [12]. A similar rounding of fracture features has been observed in fatigue of polyoxymethylene when heating of the sample occurred [13]. Even the least ductile of the blends, the dry as-moulded 25% HI–N66, possesses sufficient ductility that the resulting deformation obscures any possible evidence of pure trans-spherulitic fracture such as observed by Bretz [3]. In summary, the patchy fracture surface appearance found in the nylon blends is believed to result from microvoid formation around rubber particles at the crack tip damage zone. This microvoid formation and the associated intensive deformation results in energy dissipation, and contributes to the greater fatigue resistance of the blends as compared to the neat nylon. The random path followed by the crack through the damage zone gives rise to the large network of patches.

The transition from the patchy to the rumpled fracture surfaces occurs gradually and occurs at lower stress intensity levels with increasing water content, rubber content, and test frequency. Fig. 6 shows the effect of frequency on the fracture morphology. At the left in the photograph, the crack progressed at a test frequency of 30 Hz, and displayed a rumpled morphology. The test was stopped, the specimen allowed to cool, and the test begun again at 10 Hz. The resulting fracture morphology changed to the patchy type. Thus, it is clear that the transition from patchy to rumpled fracture is favoured by higher test frequency, associated with increased hysteretic heating at the crack tip [12].

Increases in any of these variables – water content, rubber content, and frequency – make the material more ductile at the crack tip, either by inherent changes in the material properties or by increasing the amount of hysteretic heating, which also increases the ductility of the material. Thus, variables that increase ductility also hasten the onset of the high-ductility fracture process that generates the rumpled fracture morphology. Since the rumples are parallel to the crack front, the question naturally arises as to whether these fracture bands are fatigue striations. Fatigue striations occur in many polymeric materials [1] including unmodified nylon [3], and appear as a series of parallel lines oriented perpendicular to the direction of crack growth. The spacing between these lines represents the incremental advance of the crack during a single loading cycle. If the rumples are indeed striations, measurement of their spacing should correspond on a one-to-one basis to macroscopic crack growth rate measurements.

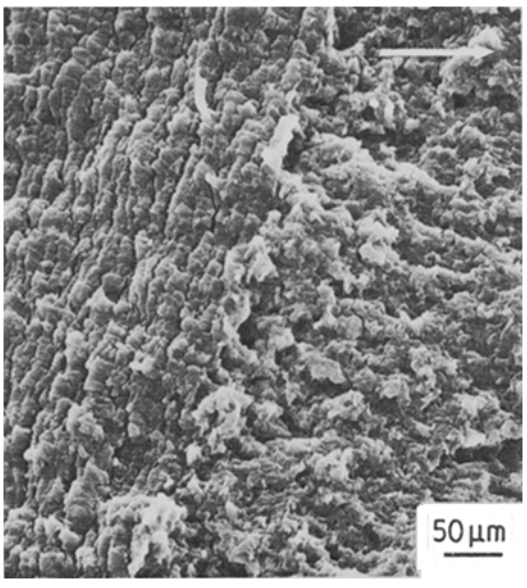

Figure 6 SEM fractograph of dry 100% HI–N66. The abrupt change in fracture morphology seen in the photo is associated with a reduction in the test frequency from 30 Hz (left of photo) to 10 Hz (right), with the sample cooled to room temperature before resuming the test at the lower frequency.

In Fig. 7 the rumple spacing is plotted as a function of the growth rate, da/dN. The dashed line in the figure represents the equality of the rumple spacing and the crack growth rate per cycle which would be expected if the rumples were, indeed, fatigue striations. Although the data and the dashed line converge at high growth rates, the rumple spacing is generally greater than the average growth increment per loading cycle. Moreover, for crack growth rates ranging over three orders of magnitude, the rumple spacings change only by an order of magnitude. The rumple formation, therefore, must reflect a fracture process which is not directly related to the macroscopic growth process. In support of this finding, it should be pointed out that the rumples are observed in fast fracture. Similar findings were reported in unmodified nylon [3], and in impact fracture studies of HI–N66 [14]. In the latter material, Flexman [14] observed rumples that were separated by fissures with fibrils spanning the fissures. (Fibrils were rarely

*It was thought that the porous appearance of the patchy fracture morphology might be due to beam damage; however, careful examination at low and high magnification showed that the image did not change with time, negating such a possibility.

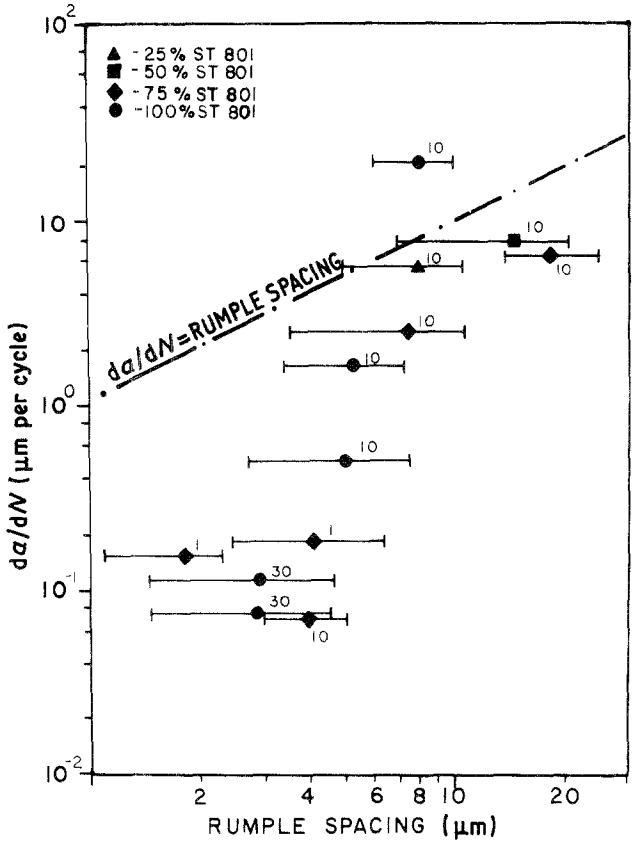

Figure 7 Plot of average measurement of rumple spacing against fatigue crack growth rate. The dashed line indicates the one-to-one correspondence expected if the rumples were striations.

observed between the rumples in the fatigue fracture surfaces in the present study, probably the result of their cyclic- induced rupture.) The width of the rumple spacings was about 2 to 10 μm. Fine lines parallel to the direction of crack growth were also seen on the rumples and were spaced about 1 μm apart.

The following model is proposed to account for the formation of the rumpled fracture surface. Since these nylon blends possess considerable ductility, they are capable of considerable drawing at the crack tip prior to unstable fracture. As the material is drawn in the Y direction along the YZ plane, there is a tendency for the material to weaken in a direction normal to this plane. The highly drawn material is then susceptible to delamination along this plane in response to the normal stress in the X direction; secondary fissures then occur in the YZ plane, parallel to the rumple bands. Crack advance then results from the linking-up of these fissures through drawing-out of the ribbons of oriented material which are surrounded by the secondary fissures (Fig. 8). It follows that rumple formation should be more pronounced at high ΔK

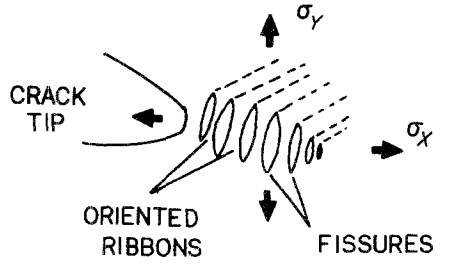

Figure 8 Schema of rumpled fracture surface formation.

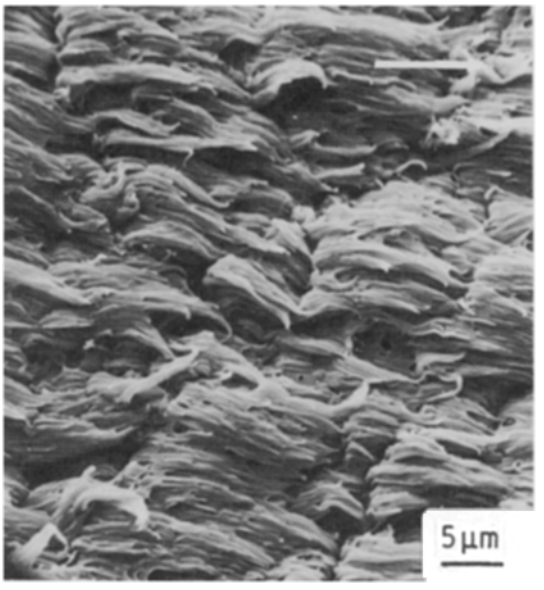

Figure 9 SEM fractograph of 100% HI–N66 showing bulbs at the end of tufts.

levels, since the associated greater degree of hysteretic heating would enhance ductility and result in more pronounced rumple formation.

The rumple formation model does not preclude rumple formation in the fast fracture region. It should be noted, however, that associated fissures found in the fast fracture region are not as deep, and tufts of material are drawn across the fissures. The reason why the rumples are less well-defined at high ΔK levels and in fast fracture may be related to the fact that there are fewer cycles for the microcracks (fissures) to form. Furthermore, the drawn tufts of material extend across the fissures, thereby further obscuring the fissures.

The tufts usually appear to be drawn to a point, but occasionally in the fast fracture region, round bulbs are seen at the ends of the tufts, as in Fig. 9. These bulbs may be the result of melting or extreme heating of the drawn tuft during the deformation and fracture process. Similar features have been observed in the fast fracture of nylon 66 fibres [13] and polystyrene [15], and in the thermally assisted fatigue failure of viscose fibres [16].

These same fracture morphologies are observed in neat nylon 66 at different test temperatures. However, for each water content the fracture morphology transition is observed at a different temperature. The dry nylon is seen to fracture in a trans-spherulitic manner at 25° C but has the drawn morphology at 52° C. For the nylon with 2.6% water, which reveals a drawn fracture morphology at room temperature, trans-sperulitic fracture occurs at temperatures of 0° C or below (Fig. 10). The fracture surface of the nylon with 4.0% water exhibits a drawn morphology at 0° C and above, but fatigue failure occurs by the trans-spherulitic mode at −33° C. Finally, nylon samples with 8.5% water exhibited a drawn fracture surface morphology at all temperatures equal to or greater than −33° C as shown in Fig. 11. When tested at −70° C, however, trans-spherulitic failure resulted as shown in Fig. 12. These results are summarized in

TABLE I Nylon 66 fracture morphology variation with temperature and water content*

Temperature (°C)	Absorbed water (%)			
	0.2	2.6	4.0	8.5
−70	–	–	–	T
−33	T	T	T	D
0	T	T	D	D
25	T	D	D	D
52	D	D	D	D

*T = trans-spherulitic appearance; D = drawn appearance.

Table I, which shows the dependence of temperature and moisture on the fractographic apppearance of nylon 66. It can be seen that the trans-spherulitic fracture surface is observed at higher levels of water, the lower the test temperature. This change in fractographic appearance reflects the change in the viscoelastic state of the nylon with temperature and water content. Comparison of the results shown in Table I with dynamic modulus data for nylon [10, 17] shows that the trans-spherulitic fracture mode is observed only when the test temperature is below the glass transition temperature T_g as measured at 110 Hz. That is, for trans- spherulitic failure to occur, the nylon must exist in the glassy state; a similar suggestion was made previously for nylon fatigue tests conducted at room temperature [3]. Thus, the change in fractographic appearance as a function of water content and temperature is really a manifestation of the effects of these two variables on the viscoelastic state of the nylon.

These fractographic results are consistent with the FCP results discussed elsewhere [11]. For a given test temperature, the minimum in growth rates as a function of water content corresponds to a favourable combination of modulus and damping. In general, this favourable combination appears to correspond to the lowest water content at which the drawn fracture morphology is observed at a given temperature. In summary, the fractographic results confirm that FCP resistance is maximized with a large modulus to minimize strain per cycle, but with the material capable of sufficient deformation at the crack tip so as to blunt the advancing crack.

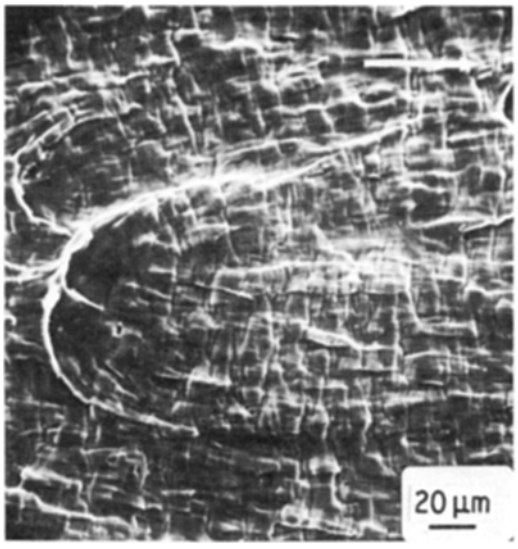

Figure 11 Fractograph of nylon 66 with 8.5% water tested at −33° C. Note drawn fracture morphology.

The fractographic studies show that the fracture morphology of nylon is related to the viscoelastic behaviour of the polymer. The specific effects of material and test variables are related, in turn, to the effects of these variables on the viscoelastic state of the nylon.

4. Conclusions

The fracture mechanisms observed in N66 and impact-modified N66 were found to depend on moisture content, level of impact modification, test temperature and frequency, and prevailing ΔK level. In most instances, the influence of these variables on fracture processes was dependent on the influence of these factors on the viscoelastic state of the nylon 66 polymer.

Acknowledgements

The authors thank the Office of Naval Research for partial support of this work, and E. I. duPont de

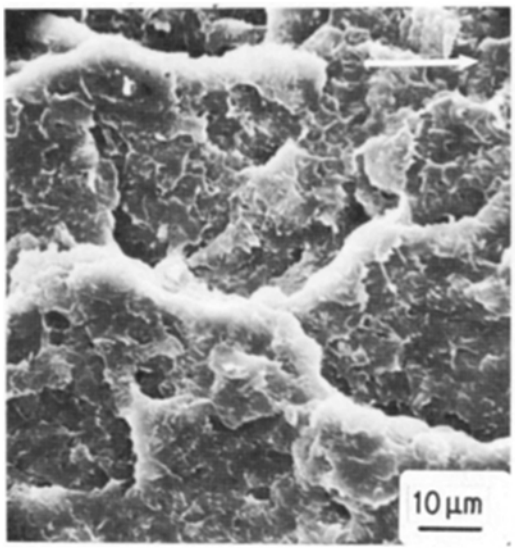

Figure 10 Fractograph of nylon 66 with 2.6% water tested 0° C. Note patchy fracture morphology.

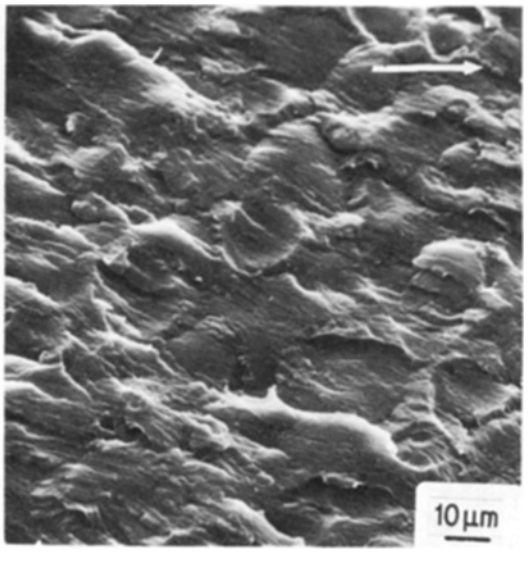

Figure 12 Fractograph of nylon 66 with 8.5% water tested at −70° C. Note patchy fracture morphology.

Nemours & Co. for providing the material supply for this study. One of the authors (M.T.H.) received partial fellowship support from the IBM Corporation.

References

1. R. W. HERTZBERG and J. A. MANSON, "Fatigue of Engineering Plastics" (Academic, New York, 1980).
2. R. W. HERTZBERG, M. D. SKIBO and J. A. MANSON, ASTM STP 675 (American Society for Testing and Materials, Philadelphia, 1979) p. 471.
3. P. E. BRETZ, PhD thesis Lehigh University (1980).
4. P. E. BRETZ, R. W. HERTZBERG and J. A. MANSON, *J. Mater. Sci.* **16** (1981) 2070.
5. J. R. WHITE and J. TEH, *Polymer* **20** (1979) 764.
6. P. E. BRETZ, R. W. HERTZBERG and J. A. MANSON, *ibid.* **22** (1981) 1272.
7. *Idem, J. Appl. Polym. Sci.* **27** (1982) 1707.
8. K. FRIEDRICH, *Fracture* **3** (1977) 1119.
9. R. W. HERTZBERG, M. D. SKIBO and J. A. MANSON, ASTM STP 700 (American Society for Testing and Materials, Philadelphia, 1980) p. 49.
10. M. T. HAHN, R. W. HERTZBERG and J. A. MANSON, *J. Mater. Sci.* **18** (1983) 3551.
11. M. T. HAHN, R. W. HERTZBERG, J. A. MANSON and L. H. SPERLING, *Polymer*, in press.
12. M. T. HAHN, R. W. HERTZBERG and J. A. MANSON, *J. Mater. Sci.* **21** (1986) 31.
13. L. ENGEL, H. KLINGELE, G. W. EHRENSTEIN and H. SCHAPER, "An Atlas of Polymer Damage" translated by M. S. Welling (Prentice-Hall, Engelwood cliffs, New Jersey, 1981).
14. E. A. FLEXMAN, Jr, Proceedings of the International Conference on Toughening of Plastics, London, July 1978 (Rubber and Plastics Institute, London) p. 14.1.
15. R. N. HAWARD and I. BROUGH, *Polymer* **10** (1969) 724.
16. J. W. S. HEARLE and I. E. CLARKE, "Fatigue '81" edited by F. Sheratt and J. B. Sturgeon (Westbury House, Guilford, Surrey, England, 1981) p. 210.
17. M. I. KOHAN, "Nylon Plastics" (Wiley–Interscience, New York, 1973) p. 318.

Received 17 December 1984
and accepted 15 January 1985